Ge *et al.*
Chinese Journal of Mechanical Engineering (2022) 35:98
https://doi.org/10.1186/s10033-022-00752-x

Chinese Journal of Mechanical Engineering

ORIGINAL ARTICLE

Open Access

Simulation and Experimental Study on Improving Electrochemical Machining Stability of Highly Convex Structures on Casing Surfaces Using Backwater Pressure

Zhenghui Ge, Wangwang Chen and Yongwei Zhu*

Abstract

Casing parts are regarded as key components of aero-engines. Most casing parts are attached to convex structures of different shapes, whose heights range from hundreds of microns to tens of millimeters. Using profiling blocky electrodes for electrochemical machining (ECM) of casing parts is a commonly adopted method, especially when highly convex structures. However, with an increase in the convex structure height, the flow fields of the machining areas become more complex, and short circuits may occur at any time. In this study, a method to improve the flow field characteristics within a machining area by adjusting the backwater pressure is proposed and validated through simulation and experiment analyses. The simulation results demonstrated that the back-pressure method can significantly improve the uniformity of the flow field around the convex structure compared with the extraction and open outlet modes. Subsequently, the back-pressure value was optimized at 0.5 MPa according to the simulation results. The experimental results showed that using the optimized back-pressure parameters, the cathode feed-rate increased from 0.6 to 0.7 mm/min, and a 16.1 mm tall convex structure was successfully machined. This indicates that the back-pressure method is suitable and effective for electrochemical machining of highly convex structures with blocky electrodes. In this study, we propose a method to improve the electrochemical machining stability of a convex structure on a casing surface using backwater pressure, which has achieved remarkable results.

Keywords: Casing parts, Electrochemical machining, Convex structures, Back-pressure method, Blocky electrode

1 Introduction

Casing parts are regarded as key aero-engine components and play an important role in connection, load-bearing, and support [1–3]. To function properly during the extreme working conditions of aero-engines, casing parts are typically made of hard-to-cut materials with excellent high-temperature performance, such as nickel-based alloys. Moreover, most casing parts are thin-walled revolving parts with complex convex structures on their outer surfaces, and their heights vary from several to tens of millimeters [4, 5]. Therefore, manufacturing these parts is a significant challenge for traditional machining methods owing to significant tool wear, high machining cost, and long machining periods [6–9].

Electrochemical machining (ECM) is a non-contact machining method based on the electrochemical dissolution of anode materials without limitations on the mechanical properties of alloys [10, 11]. Owing to the advantages of a high material removal rate, no tool wear, etc., ECM has recently become an important processing method for casing parts [12–14]. Zhu et al. proposed the so-called counter-rotating electrochemical machining (CRECM) technology [15–17]. Through the

*Correspondence: ywzhu@yzu.edu.cn

College of Mechanical Engineering, Yangzhou University, Yangzhou 225000, China

counter-rotating movement of the rotary tool electrode and workpiece, the one-time formation of a convex structure on the casing surface can be realized, which effectively improves the machining efficiency and machining quality of the casing parts. Zhang et al. carried out a research on mask electrochemical machining (M-ECM) of casing parts, achieving a few key breakthroughs such as the preparation of the protective film of the rotary surface and uniformity control of the flow field, and realized engineering applications for a certain type of casing part [18, 19]. However, to date, the above methods are mainly used for machining casing parts with relatively low convexity.

Using profiling blocky electrodes for ECM of convex structures on casing parts is a widely used method, especially for processing highly convex structures on larger-sized casing parts, owing to its high machining efficiency. Li et al. designed a series of working stations and blocky cathode tools. By matching the positions of the working stations and cathode tools, a complex concave-convex structure was gradually formed on the casing part surface [20]. Sheng et al. conducted experimental research on the ECM of a convex structure on the casing surface using a blocky electrode. Based on the experimental results, they optimized the flow field and process parameters and improved the machining quality of the casing parts [21, 22].

However, the flow field is an important factor affecting the machining performance of ECM [23, 24]. Compared with other ECM methods, such as CRECM and M-ECM, the machining area of the blocky electrode method is larger, and the uniformity of the flow field within the machining gap is more difficult to control. With an increase in the feed depth of the blocky electrode, the machining gap flow field becomes more complex; subsequently, short circuits may occur at any time. Therefore, ensuring the uniformity and stability of the flow field in the machining gap and avoiding the "dead water area" phenomenon have become the most important factors in the ECM process of a highly convex structure using a blocky electrode.

In this study, the flow field characteristics during the ECM process of highly convex structures with blocky electrodes are emphasized, and a back-pressure method is proposed to improve the flow field of the machining area. Three operation modes, namely, extraction, open, and back-pressure on the backwater outlet, were studied in detail using a computational fluid dynamics (CFD) software, and an optimized flow field state was obtained. The subsequent experimental results indicated that the back-pressure method is suitable and effective for ECM of highly convex structures with a blocky electrode.

2 Machining Principle and Flow Field Characteristics

Figure 1 shows a schematic for the electrochemical machining of a highly convex structure on the surface of a casing part with a blocky electrode. The blank of the casing part is fixed on the working table of the machine tool with a clamp. It is aligned to the proper relative position with the cathode tool via a rotating disk before machining. The electrolyte is pumped into the electrode inlet and directly delivered to the machining gap through an internal flow channel. When a stable voltage difference is applied between the cathode tool and anode workpiece, electrochemical dissolution occurs on the anode surface. The blocky cathode tool is continuously fed along the normal direction of the casing surface at a constant feed rate until the set machining depth is reached.

To realize the back-pressure machining method proposed in this study, a special block electrode was carefully designed, as shown in Figure 2. The red area signifies the main machining area and rhombic window corresponds to the non-machining area, which ensures that the anode workpiece surface forms a convex structure. The upper end of the blocky electrode has an inlet and back-water outlet. The inlet is responsible for delivering the high-speed

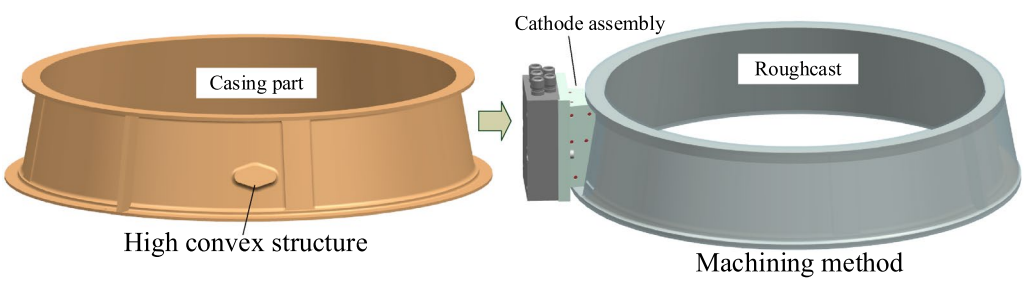

Figure 1 Schematic for electrochemical machining of a highly convex structure

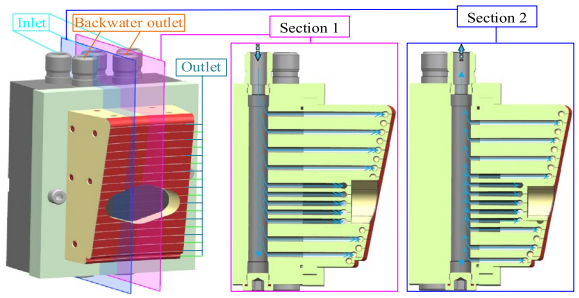

Figure 2 Schematic of a flow channel inside a cathode tool

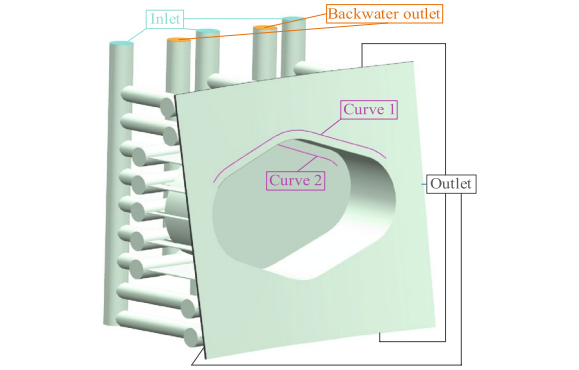

Figure 3 CFD model for ECM of a highly convex structure

electrolyte to the entire machining area. The backwater outlet is connected to the window area to adjust the flow-field state of the window area. The rhombic window is crucial for ensuring the proper formation of the convex structure. The flow field state is also complicated. Therefore, the pressure mode of the backwater outlet has a significant influence on the flow-field state of the machining gap and formation of the convex structure.

3 Theoretical Model of the Flow Field

A complex CFD model of the flow field was established, as shown in Figure 3, where the light blue area is the inlet, orange red area is the backwater outlet, and dark gray area is the outlet. To simplify the simulation process, the following assumptions are made [25]: (1) The electrolyte is assumed to be continuously flowing and incompressible. (2) The shear stress between adjacent layers of infinitesimally small fluid sections was assumed to be proportional to the rate of shear in the direction perpendicular to the motion.

The fluid flow follows conservation of momentum and mass equations, which can be described as follows:

$$\frac{\partial u_i}{\partial x_i} = 0, \tag{1}$$

$$\frac{\partial u_i}{\partial x_j} + u_j \frac{\partial u_i}{\partial x_j} = \nu \frac{\partial^2 u_i}{\partial x_j \partial x_j} - \frac{\partial p}{\partial xi} - \frac{\tau_{ij}}{\partial x_j}, \tag{2}$$

where, u_i is the ith component of the mean electrolyte, x_i is the ith cartesian coordinate, x_j is the jth cartesian coordinate, τ_{ij} is the ijth component of the stress tensor, and p and ν are the mean pressure and kinematic viscosity of the electrolyte, respectively.

In the simulation model, the electrolyte flow path was complex, and its size changes significantly. Moreover, the flow field was in a complex turbulent state. In this study, the renormalization group (RNG) k–ε turbulence model was used, which is suitable for flows with high streamline curvatures and strain rates.

The turbulence kinetic energy and dissipation rate equations for the RNG k–ε turbulence model can be described as follows:

$$\frac{\partial k}{\partial t} + u_j \frac{\partial k}{\partial x_j} = \frac{\partial}{\partial x_j}\left[\left(\nu + \frac{\nu_t}{\sigma_k}\right)\frac{\partial k}{\partial x_i}\right] + G - \varepsilon, \tag{3}$$

$$\begin{aligned}\frac{\partial \varepsilon}{\partial t} + u_j \frac{\partial \varepsilon}{\partial x_j} &= \frac{\partial}{\partial x_j}\left[\left(\nu + \frac{\nu_t}{\sigma_\varepsilon}\right)\frac{\partial \varepsilon}{\partial x_j}\right] + C_{\varepsilon 1}\frac{\varepsilon}{k}G \\ &- C_{\varepsilon 2}\frac{\varepsilon^2}{k} - C_\mu \eta^3 \frac{1-\eta/\eta_0}{1+\beta\eta^3}\frac{\varepsilon^2}{k},\end{aligned} \tag{4}$$

where, t is time, $\eta = (k/\varepsilon)(G/\nu_t)^{0.5}$, and $G = \nu_t(\partial u_i/\partial x_j + \partial u_j/\partial x_i)\partial u_i/\partial x_j$. The values of the constants are $\sigma_k = 0.7149$, $\sigma_\varepsilon = 0.7149$, $\sigma_k = 0.7149$, $\sigma_\varepsilon = 0.7149$, $C_{\varepsilon 1} = 1.42$, $C_{\varepsilon 2} = 1.68$, $C_\mu = 0.085$, $\beta = 0.012$, and $\eta_0 = 4.38$.

4 Simulation Analysis and Results

The CFD model adopted in this study is shown in Figure 3. The light-blue area is the inlet of the electrolyte, which provides the necessary pressure for the machining process. To reduce the electrolyte velocity in the convex structure area, which does not require machining, the backwater outlet is set to release the electrolyte pressure.

The parameters used in the simulation were set as follows: the inter-electrode gap was 0.5 mm, pressures of inlet and outlet were 1 and 0 MPa, respectively, extraction outlet pressure was 0.4 MPa, open outlet pressure was 0 MPa, and backwater pressure was set between 0 and 1 MPa.

4.1 Influence of Flow Mode on the Flow Field

In this study, three modes, namely, extraction outlet, open outlet, and back-pressure outlet, are designed to obtain a better flow field state. Figure 4 shows the flow field in the machining gap with an outlet pressure of 0 MPa, extraction pressure of 0.4 MPa, and back-pressure

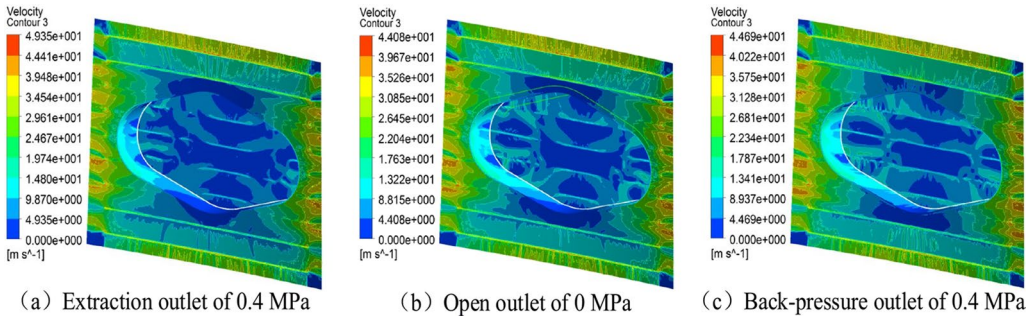

（a）Extraction outlet of 0.4 MPa （b）Open outlet of 0 MPa （c）Back-pressure outlet of 0.4 MPa

Figure 4 Electrolyte velocity distribution of machining gap with respect to different flow modes

of 0.4 MPa. It could be observed that there is an obvious low-speed area around the convex structure (especially the upper edge area) under the extraction and open outlet modes, which causes uneven corrosion in the machining area. In contrast, the flow field of the convex edge region is significantly improved when the back-pressure mode is applied. Therefore, we can conclude that the back-pressure outlet mode is beneficial for improving the flow field state of the machining gap and enhancing the uniformity and stability of the machining process compared with the extraction and open outlet modes.

4.2 Influence of Backwater Pressure on the Flow Field

In this section, the flow field of the machining gap under different back pressure values is discussed in detail. Figure 5 shows the electrolyte velocity distribution of the machining gap at back pressure values of 0.2, 0.6 and 1 MPa. It could be noticed that with an increase in the back pressure, the flow field around the convex structure also improves.

To better explain the abovementioned phenomena, we plot spline curves of the top area and surrounding area of the convex structure (as shown in Figure 3) and extract the electrolyte velocity parameters accordingly. Figure 6a shows the electrolyte velocity distribution of spline curve 1 around the convex structure with respect to different back pressure values. It could be observed that the average electrolyte velocity along curve 1 is approximately 10 m/s, which meets the demand of electrochemical machining for electrolyte velocity. However, Figure 6a also shows that the electrolyte velocity along curve 1 fluctuates significantly, especially when the back pressure is less than 0.4 MPa, and the minimum electrolyte velocity is less than 4 m/s. This is significantly lower than the electrolyte velocity requirements of ECM processes, which is approximately 10–30 m/s [26, 27]. Accordingly, this area may become dangerous owing to the possibility of short circuits under such circumstances. Furthermore, Figure 6a shows that with the increase in back pressure, the electrolyte velocity along curve 1 gradually increases and that of the dangerous area also improves accordingly. Therefore, increasing the back pressure is beneficial for maintaining the stability of an ECM process.

Figure 6b shows the electrolyte velocity distribution of spline curve 2 in the top area of the convex structure with different back pressure values. It should be noted that the top area of the convex structure is a non-machining area; therefore, a lower electrolyte velocity should be employed to avoid stray corrosion and enhance the forming height of the convex structure. As shown in

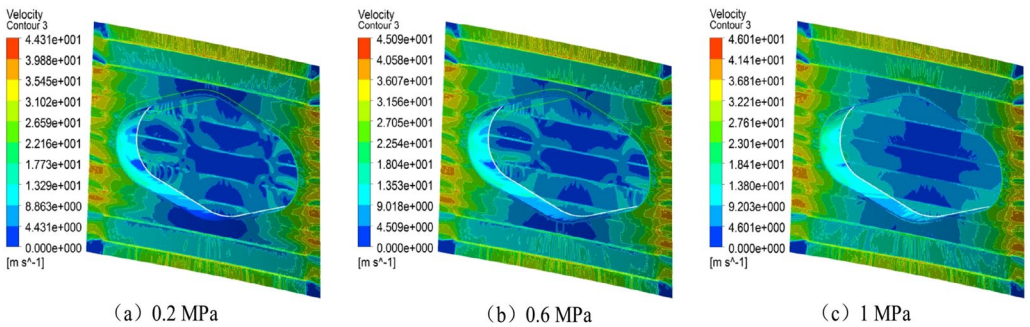

（a）0.2 MPa （b）0.6 MPa （c）1 MPa

Figure 5 Electrolyte velocity distribution of machining gap with respect to different back pressure values

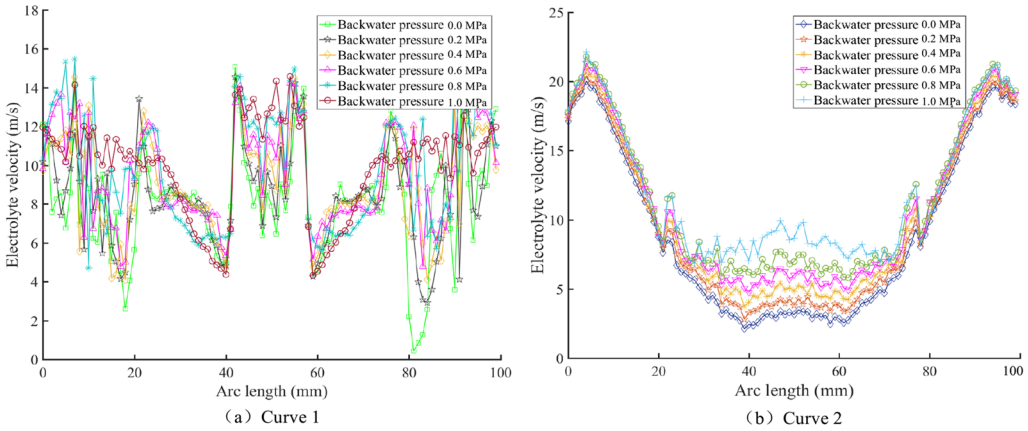

Figure 6 Electrolyte velocity distribution contours in the convex structure area of a machining gap

Figure 6b, with an increase in back pressure, the electrolyte velocity increases gradually. When the back pressure value exceeds 0.6 MPa, the electrolyte velocity is greater than 5 m/s. This exceeds the minimum electrolyte velocity of 4 m/s on the machining area of curve 1. Consequently, we can assume that there will be more stray corrosion to the top area of the convex structure. In summary, the back-pressure method can improve the flow field state of the machining gap; however, using a too high back pressure value will cause excessive stray corrosion in the top area of the convex structure, which is undesirable during the process. Therefore, a back pressure value of 0.5 MPa will be applied preferentially in the following experiments.

5 Experimental Verification

To further verify the effectiveness of the method proposed in this study, ECM processes of highly convex structures on a certain casing part surface were conducted in controlled experiments. The experimental setup consisted of a tool motion control system, electrolyte circulation system, power supply system, and current direction system, shown in Figure 7a. The cathode fixture was made of fiber-reinforced plastic material, whereas the workpiece fixture was made of stainless-steel material. The assembly site for the machining process is shown in Figure 7b. During the machining process, the open outlet pressure was kept constant at 0 MPa, and the backwater pressure outlet was adjustable. The experimental conditions and parameters are presented in Table 1.

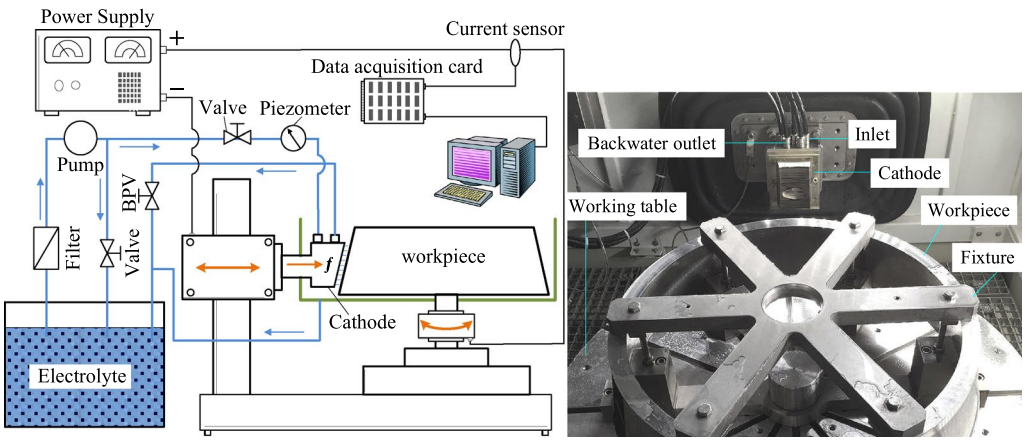

Figure 7 **a** Schematic of the experimental setup, **b** Assembly site for the ECM process

Table 1 Experimental conditions

Parameter	Value
Workpiece material	Nickel-based superalloy
Cathode material	Stainless steel
Applied voltage (V)	30
Electrolyte inlet pressure (MPa)	1
Electrolyte outlet pressure (MPa)	0
Backwater outlet pressure (MPa)	0.5
Electrolyte conductivity (mS/cm)	150
Electrolyte temperature (℃)	30

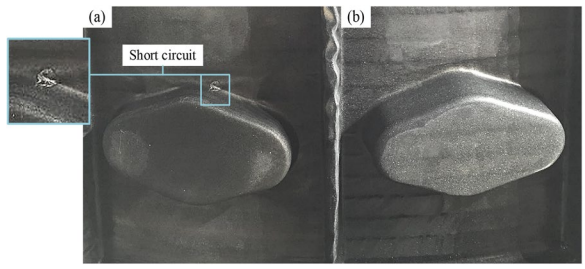

Figure 8 The machined samples: **a** open outlet mode with a feed rate of 0.6 mm/min, **b** back-pressure outlet mode with a feed rate of 0.7 mm/min and back pressure of 0.5 MPa

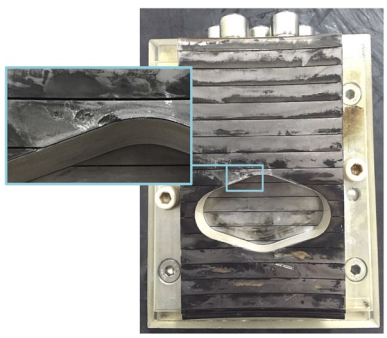

Figure 9 Short circuit region of the cathode under open outlet mode with a feed rate of 0.6 mm/min

Figure 8 shows the machined samples under different conditions. For the sample machined under the open outlet mode with a feed rate of 0.6 mm/min, a short circuit occurred when the feed amount was deep, as shown in Figure 8a. The blocky electrode tool was also damaged as shown in Figure 9. Figure 10 shows the current signal collected during machining. It can be observed that the machining time was approximately 14 min, and the corresponding convex structure height was approximately 8.4 mm, which is significantly higher than that obtained

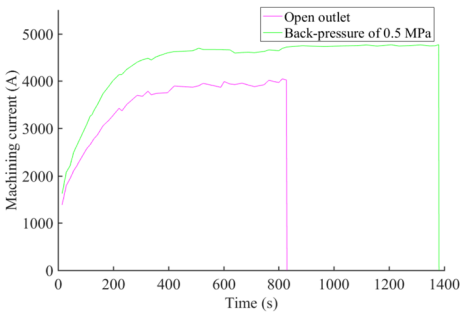

Figure 10 Variations in the experimental machining currents

by other electrochemical machining methods such as CRECM and M-ECM [10, 11]. This illustrates that the blocky electrode method has a significant advantage in machining highly convex structures on the surface of casing parts

Figure 8b shows the sample machined under the back-pressure mode with a back pressure value of 0.5 MPa. The feed rate was increased to 0.7 mm/min and machining time was extended to 23 min. The forming height of the convex structure was approximately 16.1 mm, which was more than twice the forming height of the open outlet mode. Moreover, the forming contour was very sharp. The results indicate that the back-pressure method can significantly improve the stability during the electrochemical machining of a highly convex structure with a blockly electrode and greatly increase the forming height of the convex structure. This conclusion agrees well with the simulation results obtained in Section 4, which further proves that the back-pressure method is feasible and reliable for ECM of a highly convex structure using a blocky electrode.

6 Conclusions

(1) Simulation experiments regarding three modes were performed. The results demonstrated that the back-pressure mode can significantly improve the uniformity of the flow field around the convex structure and eliminate potentially dangerous areas compared with the extraction and open outlet modes.

(2) The back-pressure mode was studied in detail. The results indicated that with an increase in the back pressure, the flow field around the convex could be significantly improved. However, the velocity at the top of the convex was significantly increased as well, which may aggravate unnecessary stray corrosion. Then, an optimized back pressure value of

0.5 MPa was obtained according to the simulation results, which realized a uniform and stable distribution of the flow field in the machining area.

(3) Experiments were conducted to verify the effectiveness of the simulation results. The experimental results demonstrated that under the optimized back pressure conditions, the cathode feed-rate increased from 0.6 to 0.7 mm/min, and an approximately 16.1 mm tall convex structure could be successfully machined. The results indicated that the back-pressure method was suitable and effective for electrochemical machining of highly convex structures with blocky electrodes.

Acknowledgements
Not applicable.

Author Contributions
ZG was responsible for all analyses and wrote the original version of the manuscript; WC provided the numerical model and performed the simulations; WZ provided guidance on the write of manuscript. All authors read and approved the final manuscript.

Authors' Information
Zhenghui Ge, born in 1980, is currently an associate professor at *College of Mechanical Engineering, Yangzhou University, China*. He received his PhD degree from *Nanjing University of Aeronautics and Astronautics, China*, in 2018. His researches mainly focus on electrochemical machining.
Wangwang Cheng, born in 1997, is currently a postgraduate student at *College of Mechanical Engineering, Yangzhou University, China*.
Yongwei Zhu, born in 1966, is currently a professor at *College of Mechanical Engineering, Yangzhou University, China*. He received his PhD degree from *Nanjing University of Aeronautics and Astronautics, China*, in 2000.

Funding
Supported by National Natural Science Foundation of China (Grant No. 51775484), and China Postdoctoral Science Foundation (Grant No. 2020M670791).

Competing Interests
The authors declare no competing financial interests.

Received: 20 February 2021 Revised: 22 May 2022 Accepted: 24 May 2022
Published online: 28 July 2022

References

[1] J Wang, M Luo, B H Wu, et al. A trochoidal path planning method of cycloid rough machining trajectory of aeroengine casing. *Acta Aeronuaut Astronuut Sinnica*, 2018, 39(6): 216-227.
[2] D Y Wang, Z W Zhu, B He, et al .Counter-rotating electrochemical machining of a combustor casing part using a frustum cone-like cathode tool. *Journal of Manufacturing Processes*, 2018, 35: 614-623.
[3] E Poursaeidi, A Kavandi, K Vaezi, et al. Fatigue crack growth prediction in gas turbine casing. *Engineering Failure Analysis*, 2014, 44: 371–381.
[4] C M Wang. *Machining technology of casing*. Beijing: Scincece Press, 2018. (in Chinese)
[5] B He, D Y Wang, Z W Zhu, et al. Research on counter-rotating electrochemical machining of convex structures with different heights. *The International Journal of Advanced Manufacturing Technology*, 2019, 104(19): 3119-3127.
[6] S Bolsunovskiy, V Vermel, G Gubanov, et al. Thin-walled part machining process parameters optimization based on finite-element modeling of workpiece vibrations. *Procedia CIRP*, 2013, 8: 276-280.
[7] Y Y Gao, J W Ma, Z Y Jia, et al. Tool path planning and machining deformation compensation in high-speed milling for difficult-to-machine material thin-walled parts with curved surface. *The International Journal of Advanced Manufacturing Technology*, 2016, 84: 1757-1767.
[8] J Kohler, T Grove, O Maib, et al. Residual stresses in milled titanium parts. *Procedia CIRP*, 2012, 2: 79–82.
[9] R M'saoubi, D Axinte, S L Soo, et al. High performance cutting of advanced aerospace alloys and composite materials. *CIRP Annals*, 2015, 64(2): 557–580.
[10] F Klocke, M Zeis, A Klink, et al. Experimental research on the electrochemical machining of modern titanium- and nickel-based alloys for aero engine components. *Procedia CIRP*, 2013, 368-372.
[11] J Sun, W Chen, J L Song, et al. Fabrication of superhydrophobic micro post array on aluminum substrates using mask electrochemical machining. *Chinese Journal of Mechanical Engineering*, 2018, 31(1): 1-7.
[12] K P Rajurkar, D Zhu, J A Mcgeough, et al. New developments of electrochemical machining. *CIRP Annals*, 1999, 48(2): 567–579.
[13] Y D Wang , Z W Zhu , N F Wang , et al. Effects of shielding coatings on the anode shaping process during counter-rotating electrochemical machining. *Chinese Journal of Mechanical Engineering*, 2016, 29(5): 971-976.
[14] Y C Ge, Z W Zhu, D Y Wang. Electrochemical dissolution behavior of the nickel-based cast superalloy k423a in $NaNO_3$ solution. *Electrochimica Acta*, 2017, 253: 379-389.
[15] Z W Zhu, D Y Wang, J Bao, et al. Cathode design and experimental study on the rotate-print electrochemical machining of revolving parts. *The International Journal of Advanced Manufacturing Technology*, 2015, 80: 1957-1963.
[16] D Y Wang, Z W Zhu, D Zhu, et al. Reduction of stray currents in counter-rotating electrochemical machining by using a flexible auxiliary electrode mechanism. *Journal of Materials Processing Technology*, 2017, 239: 66-74.
[17] D Y Wang, Z W Zhu, H R Wang, et al. Convex shaping process simulation during counter-rotating electrochemical machining by using the finite element method. *Chinese Journal of Aeronautics*, 2016, 29(2): 534-541.
[18] H Y Li, M Q Zhang, J Feng, et al. Development and application of mask electrochemical machining technology. *Aviation Manufacturing Technology*, 2015, 58(23): 57-60.
[19] Z F Pan, M Q Zhang, X Y Cheng, et al. Research on high efficient electrochemical machining technology of gyroscopic processing complex concavo-convex and large moulding surface. *Aeronautical Manufacturing Technology*, 2012, 1: 108-111.
[20] N H Li. Electrochemical machining and application of engine case profile. *Electrical Machining and Mould*, 2020, 2: 49-51.
[21] W J Sheng, B Xu. Technological test of electrochemical machining of aero-engine casing. *Electromachining Mould*, 2010, 2: 52-59. (in Chinese)
[22] B Xu, W J Sheng. Experimental study on electrochemical machining of casing profile. *Electromachining Mould*, 2011, 4: 40-42.
[23] J Z Li, D Y Wang, D Zhu, et al. Analysis of the flow field in counter-rotating electrochemical machining. *Journal of Materials Processing Technology*, 2019, 275: 116323.
[24] L Tang, X Feng, K G Zhai, et al. Gap flow field simulation and experiment of electrochemical machining special-shaped inner spiral tube. *International Journal of Advanced Manufacturing Technology*, 2019, 100: 2485-2493.
[25] D Zhu, D Zhu, Z Y Xu, et al. Investigation on the flow field of W-shape electrolyte flow mode in electrochemical machining. *Journal of Applied Electrochemistry*, 2010, 40(3): 525-532.
[26] X L Fang, N S Qu, Y D Zhang, et al. Effects of pulsating electrolyte flow in electrochemical machining. *Journal of Materials Processing Technology*, 2014, 214(1): 36-43.
[27] Y C Ge, Z W Zhu, Z Ma, et al. Tool design and experimental study on electrochemical turning of nickel-based cast superalloy. *Journal of the Electrochemical Society*, 2018, 165(5): E162-E170.